This article has been accepted for publication in a future issue of this journal, but has not been fully edited. Content may change prior to final publication. Citation information: DOI 10.1109/ACCESS.2021.3138050, IEEE Access

Date of publication xxxx 00, 0000, date of current version xxxx 00, 0000.

Digital Object Identifier

Grape Leaf Diseases Identification System Using Convolutional Neural Networks and LoRa Technology

ZINON ZINONOS[1], SOCRATIS GKELIOS[2], ALA F. KHALIFEH[3], DIOFANTOS G. HADJIMITSIS[4], YIANNIS BOUTALIS[2], SAVVAS A. CHATZICHRISTOFIS[1]

[1]Intelligent Systems Lab, Department of Computer Science, Neapolis University Pafos, 2 Danais Avenue, 8042 Pafos, Cyprus
[2]Department of Electrical and Computer Engineering, Democritus University of Thrace, Kimmeria, Xanthi, 67100, Greece
[3]Electrical and Communication Eng. Department, German Jordanian University, Amman, 11180, Jordan
[4]Department of Civil Engineering and Geomatics, Cyprus University of Technology, Limassol CY-3036, Cyprus

Corresponding author: Zinon Zinonos (e-mail: zinon.zinonos@nup.ac.cy).

ABSTRACT Image transmission over Low-Power Wide Area Networks (LP-WAN) protocols has always been a difficult task since it necessitates high data rates and high energy consumption. Long Range (LoRa) is one such protocol, which is excellent for transferring data over long distances but has generated severe doubts regarding the viability of image transmission due to its low data rate. This paper demonstrates the application results of an integrated LoRa and Deep Learning-based computer vision system that can efficiently identify grape leaf diseases using low-resolution images. In particular, the focus in this paper is to combine the two technologies, LoRa and Deep Learning, to make the transmission of the images and the identification of the diseases possible. To achieve this objective, the framework utilizes a combination of on-site and simulation experiments along with different LoRa parameters and Convolutional Neural Model (CNN) model fine-tuning. Based on the evaluation, the proposed framework proved that the transmission of images using LoRa is possible within the protocol limitations (such as limited bandwidth and low duty cycle). Our fine-tuned model can efficiently identify grape leaves diseases. The technique is both efficient and adaptive to the specifics of each leaf disease, while it does not need any training data to adjust parameters. It is worth noting that today, end-user trust in Machine and Deep Learning models has increased significantly because of novel solutions in the field of Explainable Artificial Intelligence (XAI). In this study, we use the Grad-CAM method to visualize the output layer judgments of the CNN. The disease's spot region is highly activated, according to the visualization findings. This is how the network distinguishes between different grape leaf diseases.

INDEX TERMS CBIR, CNN, Deep Convolutional Features, Deep Learning, Global Features, Image Retrieval, LoRaWAN, Local Features

I. INTRODUCTION

The Internet of Things (IoT) allows millions of devices to be connected, measured and monitored simultaneously. Currently, billions of devices are connected and create a vast network used in different application domains to support better decision-making. IoT has been integrated into most sectors such as transportation, health care, smart cities, agriculture, manufacturing, and environmental monitoring systems, allowing advancing the device systems and technologies behind them.

Nowadays, the rising demand for automation and advanced agricultural techniques has led to many attempts to adopt the proper IoT technology on farming [1]. This technology allows the farmers to monitor their fields (e.g., temperature, moisture, crop condition, etc.) via a grid of connected sensors remotely, through the internet, from anywhere in the world. Deploying a real-time environmental monitoring system to monitor a private farm can help increase production and improve the quality of the product. Additionally, remote monitoring systems allow farmers to monitor the pest population remotely. Information acquired from the fields has been proved essential for proper decision making and pest management against various threats for the plants [2]. An agriculture application that IoT technology could be of

This article has been accepted for publication in a future issue of this journal, but has not been fully edited. Content may change prior to final publication. Citation information: DOI 10.1109/ACCESS.2021.3138050, IEEE Access

great value is grape leaf disease identification. This type of application can be done by sending data from the field using the IoT infrastructure and processing the data at the back-end using Deep Learning techniques. Early identification of grape diseases can theoretically minimize losses, control costs, and increase goods' quality.

To ensure the successful operation of such systems, a set of requirements should be satisfied. Briefly, these requirements contain conditions related to the distance of the IoT devices and the devices' energy consumption to operate for more extended periods and the low cost of building and operating such systems. A key component to meet these requirements is the communication protocol used. Over the years, several wireless communication protocols have been adopted by academia and industry, all having their advantages and drawbacks. For example, some wireless communication systems include short-range with high data rate (Wi-Fi), short-range with low data rate (ZigBee, Bluetooth), and long-range with high data rate, e.g., cellular networks (2G, 3G, 4G, 5G). For example, ZigBee and Bluetooth are not adapted for scenarios that require long-range communications. On the other side, cellular technologies can provide long-range communications but consume more energy; therefore, they are not acceptable for such IoT applications.

On the other hand, Low-Power Wide Area Networks (LPWAN) are wireless technologies with characteristics such as large coverage areas, low bandwidth, possibly small packet and application layer data sizes, and long battery life operation. LPWAN is the wireless communication technology to support IoT applications' requirements, as mentioned above. The three LPWAN leading technologies that compete for large-scale IoT deployment are the LoRa/LoRaWAN, Sigfox, and Narrowband Internet of Things (NB-IoT) [3].

LoRa is a low-power, long-range wireless technology platform that uses an unlicensed radio spectrum for industrial, scientific, and medical (ISM) purposes. Because of its open and straightforward protocol stack and its deployment and management flexibility, LoRa has recently gained much attention in the Internet of Things community. Many applications use LoRa as the communication protocol to transfer the sender's data to the receiver node. The selection of LoRa protocol by several applications was based on the fact that it operates on an open license-free spectrum, has high coverage in open space, and is relatively power consumption efficient [4]. Although LoRa has many advantages, it also has some limitations that create many research challenges. One such limitation is the maximum percentage of time in which the LoRa device can use a channel, known as duty-cycle. In European Union, using the frequency of 868MHz, a node's maximum duty cycle is 1%, meaning that a node can only be active for 36sec/hour.

Although LoRa technology has found wide application mainly in remote monitoring applications where the amount of data sent is periodic and limited, in this work, our goal is to study if LoRa technology could be used in applications with demanding communication requirements such as sending an image of a grape leaf from a vineyard to identify diseases in grape leaves. The major challenge of using LoRa is to send the image from the crops to the back-end efficiently, meaning to receive the image with an acceptable quality (based on the packet loss) enough to proceed with the identification of leaf disease and at the same time to meet the duty cycle limitation of 1%.

A. MOTIVATION/SUMMARY OF CONTRIBUTION

This paper presents a framework that combines the two disruptive technologies, LoRa and Deep Learning, on transmitting images depicting grape leaves and identifying possible diseases.

Several recent studies have raised serious questions about image transmission over the LoRa network because images need a large amount of data and consume more energy during transmission. Considering the last comment, the first goal of this paper is to evaluate the process of image transition over the LoRa network. We examine the impact of several factors throughout our simulations, such as the spreading factor, distance, and packet losses.

Image transmission over LoRa results in packet losses and major visual corruption of the images. For this study's purpose, a simulation tool has been developed to construct the received images from the gateway. In addition, a performance evaluation of a LoRa-based pilot is conducted. The pilot was implemented to monitor grape leaf for diseases in a vineyard. A LoRa pilot was set up in a rural area to evaluate its performance and extract the best LoRa parameters. The pilot results were integrated into our simulation tool.

Finally, the paper implements a plug-n-play approach for automatic grape leaf disease identification on visually corrupted and low-quality images. A Convolutional Neural Network (CNN) model effectively classifies grape leaf images into one of the four classes (Black rot, Esca, Leaf blight, and Healthy). The first class corresponds to the healthy leaf, while the three remaining classes correspond to possible diseases. The procedure is repeated for two different scenarios. In the first scenario, we use high-quality images compared to the second scenario, where we use images with lower quality and missing values due to packet losses. For this task, we employed a pre-trained CNN model and fine-tuned the architecture in our dataset. The expression plug-n-play applies to and explains two crucial aspects of the process at the same time. The first feature is that pre-trained networks can recognize gape leaf diseases without the need for any setup, preparation, or fine-tuning. This emphasizes the reusability of the pre-trained networks and their universality and ability to generalize to previously unknown data. At the same time, the word "plug-and-play" describes a critical aspect of implementation ease.

It is worth mentioning that, to the best of our knowledge, this is the first research work to demonstrate that transmitting images to identify grape leaf diseases using LoRa is feasible within protocol constraints (such as limited data rates and low duty cycle).

This article has been accepted for publication in a future issue of this journal, but has not been fully edited. Content may change prior to final publication. Citation information: DOI 10.1109/ACCESS.2021.3138050, IEEE Access

The paper is organized as follows. Section II presents the related work directly related to this paper. Section III analyses the system architecture, pilot used in this work and highlights the proposed scenario. In Section IV, the authors evaluate the proposed scenario and present collected results. Finally, the conclusions of the study are summarized in Section V.

II. RELATED WORK

A. IOT ENVIRONMENTAL MONITORING

IoT environmental monitoring is a long-studied field with a significant amount of contributions over the last decade. LoRaWAN has been used in numerous applications such as smart cities, smart farming, and environmental monitoring [5]. One example of environmental monitoring is presented in [6], where the authors deployed environmental monitoring sensors on the roof of buildings in an urban setting. In [7] a group of researchers from Finland experimented with the node located on both grounds and water in the city of Oulu. They observed that the maximum communication range on the ground was 15 km and 30 km on water. Another example of air pollution and weather monitoring system for urban areas is presented in [8]. In their study, a Vehicle Monitoring System (VMS) based on the IoT technique is developed. Different sensor modules measure the parameters and collect the measured data (Global Position System (GPS) positions, weather parameters, vehicle information, and air quality information). These parameters are then transmitted to a cloud server through the LoRa protocol. A user interface is used to show the sensing data that is stored in a cloud server. Additionally, the collected data were instantly shown on the user interface. Furthermore, in [9], the authors proposed an intelligent agricultural service platform that is based on a wireless sensor network and LoRa communication technology. This work uses LoRa as a network transmission interface to solve the problem of communication failure and save energy. Thus, an agricultural intelligent agriculture service platform is developed to support environmental monitoring and improve agricultural management efficiency.

In [10], the authors provide an analysis of the impact of variant physical layer parameters on the performance of LoRa networks in a tree farm. Overall, the LoRa communication range was smaller than the theoretically expected range. Some PHY factors, spreading Factor and coding rate, showed a clear impact on LoRa performance. Actual data reliability was inconsistent at varying distances and PHY configurations, unlike the consistency found in the Received Signal Strength Indicator (RSSI) reported by the radios.

In [11], authors present an approach for a low-cost crop sensing that is based on temporal variations of the signal strength of low-power IoT radio communication. Based on real-world experiments in wheat fields, they have shown that a significant correlation between Leaf Area Index (LAI) and RSSI time series.

In [12], authors focused on the transmission performance of LoRa technology and applied it to Sailing Monitoring System. The measurements were conducted in Brazil Olympics sailing venue for two cases, and the system's performance of coverage and packet loss rate in the sea area were analyzed. It shows that the system based on LoRa technology can achieve the intended purpose of system design and meet the essential requirement of system applications.

In [13], the authors highlight that the temperature can have a significant impact on LoRa's communication performance and demonstrate that an increase in temperature can be sufficient to transform a perfect LoRa link into an almost useless one.

The authors in [14] conducted a study to analyze the best Spreading Factor (SF) used in various distances, using the 925 MHz Industrial, Scientific, and Medical (ISM) frequency band in Indonesia. Their experiments show SF7 is the best Spreading Factor for maximum throughput, SF8 for a balance of high throughput and long-range capabilities, and SF11 for maximum range and optimal range for LoRa application. Finally, in [15] authors focus on rescue monitoring. Their goal is to study if LoRa technology can be used for such kinds of applications. The obtained simulation and real-time experiments results indicate that LoRa could be an ideal candidate for rescue monitoring.

In regards to the image transmission using LoRa, little research has appeared in the literature in the last couple of years. This topic is relatively new and quite challenging due to the technology limitations. In [16], authors presented a low-cost, long-range image surveillance system that was based on an image compression technique that can run on limited memory platforms. Based on their evaluation of this technique, the image can be transmitted up to 940 meters using LoRa. However, this work lacks a detailed performance evaluation of LoRa protocol since it is not clear the effects of different LoRa settings, such as the Spreading Factor, on the delivery of the image.

The authors in [17] used Joint Photographic Experts Group (JPEG) and JPEG 2000 methods for image compression to achieve an acceptable compression and image reconstruction while transmitting in a low-speed network such as LoRa. Based on the evaluation, the format of JPEG 2000 compression is suitable for image compression over LoRa technology. Although the authors considered the different settings of the LoRa protocol, they did not consider the duty cycle limitation, which means that no results on the total time taken to deliver the image are provided.

In [18], authors proposed a new method for mangrove forest monitoring in Malaysia, wherein they transfer image sensor data over LoRa in a node-to-node network model. To do so, they produced a scheme where the images collected by the sensor are encrypted as hexadecimal data and then split into packets for transfer via the LoRa communication link. To evaluate their solution, they measured the packet loss rate, the Peak Signal-to-Noise Ratio (PSNR), and the Structural Similarity (SSIM) index of each image. As a result, they concluded that LoRa is an ideal technology for implementing a WSN for monitoring mangrove forests. Despite that, the number of images sent and experiments performed are too small to draw robust conclusions.

In [19], the authors proposed a Carrier Sense Multiple Access (CSMA) mechanism adapted to LoRa networks for successful long-range data transmission. The purpose of this work was to evaluate the new mechanism and prove that it can eliminate collisions and, therefore, packet losses when transmitting large volumes of data such as an image.

In [20], the authors introduce a novel system to transmit a sequence of images captured from a camera on a static environment through LoRa. Their key challenge was to reduce the amount of transmitted data while preserving image quality. To this end, they developed a technique that splits an image into grid patches and transmits only the modified area of an image based on their dissimilarity measure.

B. PLANT DISEASE IDENTIFICATION

Identifying crop diseases opportunely with high precision plays a vital role in the field of agriculture as it affects productivity and food security worldwide. Therefore, it is crucial to detect the disease in time and take precautions to prevent unnecessary resources.

Various diseases affect plants with severe repercussions in the economy and agriculture. However, detection is usually performed manually with visual inspection and lab tests. As a result, this process is time-consuming and can lead to an incorrect diagnosis.

To overcome these obstacles, machine-learning methods have been applied. The first studies of plant disease detection were focused on low-level image features such as color, shape, texture, and traditional machine learning algorithms such as k-nearest neighbors, Support Vector Machines (SVM), and decision trees. In [21], plant diseases classification that requires image segmentation, followed by feature extraction of color and texture to train the classifier, is presented. The authors in [22] proposed a digital image-based algorithm to identify plant diseases that consist of color transformations, histograms, and a pairwise-based classification system. The methods in [23] and [24] are based on Global Thresholding algorithms to segment the diseased parts of the grape leaves and feed them to machine learning classifiers. These approaches, though, have severe limitations such as:

- Low-level features lack discriminative power and can only be effective with a fusion of different features
- Traditional machine learning algorithms cannot process the spatial information of the image effectively

Deep Learning (DL) and specifically CNNs have the potential to overcome these issues presented above. Deep Learning-based approaches are increasing with high pace and have been incorporated in various computer vision applications successfully. CNNs can learn relevant, class-specific features at different levels mimicking how the human brain perceives the images. CNNs topology consists of layers, maintaining a hierarchy structure starting from the input layer, followed by the hidden layers, and eventually ending in the output layer. Each layer can exploit spatial or channel information using multiple convolutional kernels with learnable weights. The multilayered, hierarchical structure of deep CNNs enables them to extract low-level features such as edges and blobs in the initial layers and, based on these, to detect higher-level features at subsequent layers [25]. As we move more in-depth, the feature hierarchies become increasingly more powerful.

The emergence of another field of machine learning, transfer learning, gave a massive boost in CNNs adoption as it relaxed the necessity of a large amount of data to train them effectively. The experimental results of [26] emphasized pre-trained CNNs capability to form robust baselines. Therefore, most of the recent studies in leaf disease classification use DL methods as their primary approach.

The authors in [27] adopted a modified version of the popular CNN architecture AlexNet to identify cucumber leaf disease. The proposed method consists of three main adjustments:

1) The fully connected layers are replaced with a global pooling layer
2) Dilated convolutional layers are adopted
3) Combination of global pooling and dilated convolution are used

The S-CNN approach [28] proposed the extraction of random patches from each image, followed by an augmentation step. In the last stage, augmented patches feed the CNN. The model that utilized the segmented images outperformed the model trained with the full images. In a similar vein, a more sophisticated approach is presented in [29]. The proposed approach is a two-step process. The first step includes the segmentation of leaves from the background using a U-Net architecture. In the second step, classification is performed, extracting high-level features from pre-trained CNNs. Afterward, popular pre-trained architectures are compared regarding their classification performance, emphasizing the segmentation module's importance for plant disease recognition. The Plant Disease Diagnosis and Severity Estimation Network (PD2SE-Net) [30] is another DL approach for plant disease diagnosis. Residual Network (ResNet) [31] architecture is employed as a backbone incorporating shuffle blocks to reduce the computational complexity efficiently.

III. THE PROPOSED APPROACH

Our proposed system architecture is shown in Fig. 1. The system consists of three main components: the LoRa pilot, the simulator, and the pre-trained CNN network.

A. LORA

LoRa is a wireless modulation for long-range, low-power, and low-data-rate applications developed by Semtech and belongs to the LPWAN family. LoRa allows long-range communications at a low bit rate among the connected objects (things) wirelessly.

This article has been accepted for publication in a future issue of this journal, but has not been fully edited. Content may change prior to final publication. Citation information: DOI 10.1109/ACCESS.2021.3138050, IEEE Access

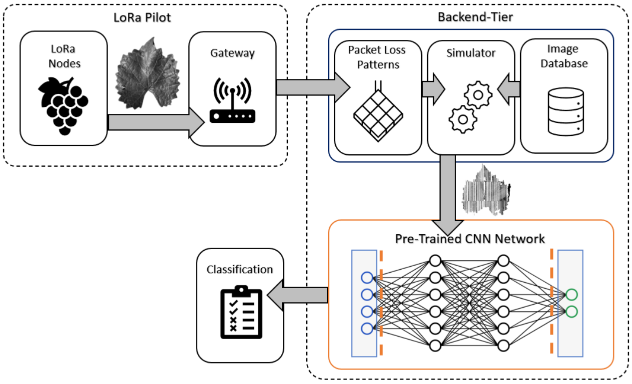

FIGURE 1: System Architecture

LoRa allows the configuration of four critical parameters, Bandwidth (BW), Spreading Factor, Coding Rate (CR), and Transmit Power (TXP).

- Bandwidth: it is the width of the transmitted signal. It can only be chosen among three options: 125 kHz, 250 kHz, or 500 kHz. 125 kHz must be configured for a long-range transmission, where 500 kHz is used for fast transmission.
- Spreading Factor: it refers to a value that determines how to spread the chirp. In LoRaWAN networks, SF7 to SF12 is used in a step of 1. The selection of SF also defines the data rate. Table 1 presents the chirp packet length based on the SF parameter. Modifying this parameter provides a trade-off between increasing the communication distance and decreasing the data transfer rate.
- Coding Rate: an error correction code added to a packet before transmission. To calculate the CR, the following formula is used:

$$CR = \frac{4}{4+n}, n = 1, 2, 3, 4 \tag{1}$$

  where n is the number of redundant bits.
- Transmission Power: Transmission Power is the amount of power used to transmit a chirp. The higher is the transmission power, the higher the power consumption. For example, for the transmission power of 20 dBm, the power consumption is 412.5 mW.

TABLE 1: LoRa Data Rates [32]

Data Rate (DR)	Spreading Factor	Bandwidth (kHz)	Max App Payload (bytes)
0	12	125	51
1	11	125	51
2	10	125	51
3	9	125	115
4	8	125	222
5	7	125	222

B. LORA PILOT

The pilot's main purpose is to receive images from a private farm field from six nodes placed at different distances from the gateway, scattered to a field of grapes crops.

- Node: in the presented experiments, we use an Arduino UNO microcontroller which is based on the ATmega328 architecture.
- Transceiver: we use the Dragino LoRa Shield, which allows the user to send data and reach extremely long ranges at low data rates. It provides ultra-long range Spread Spectrum (SS) communication and high interference immunity whilst minimizing current consumption. LoRa shield is based on Semtech SX1276/SX1278 chip.
- Gateway: we use the LG01-N gateway by Dragino. LG01-N features an open-source, OpenWrt system, single-channel LoRa gateway. It allows users to send data at low data rates but reaching extremely long ranges.

The pilot was set up in a rural area in Rhodes Island and, more specifically, in the South Aegean region plant nursery in Greece. We employed the LoRa network composed of a gateway and six nodes to send the image packets to the gateway. One of the nodes was placed at the farthest crop area (600 m) with line-of-sight to the gateway; another node was located to 200 m (line-of-sight) from the gateway and, finally, the remaining nodes were employed closer to the gateway but with natural obstacles between their communication path to the gateway. Nodes 1 to 4 are located closer to the gateway but with natural obstacles between their communication path to the gateway where nodes 5 and 6 were placed in position with line-of-sight to the gateway. The purpose is to investigate the performance of the pilot and, more specifically, how different LoRa settings affect the Packet Reception Rate (PRR) and, therefore, the reception of the image data. Further to the PRR, we investigate the behavior of the RSSI, Signal-Noise Ratio (SNR), and uplink delay of the image data. In addition, we explore how weather temperature affects the RSSI.

For each node, 50 images were sent by changing every time the spreading Factor (from 7 to 12). The bandwidth was set to 125 kHz, transmission power to 14 dBm, and finally, the coding rate to 4/5. To reduce the size of the transmitted data and the LoRa overhead, we transformed the images to grayscale. By doing this, for an image of 255×255 bytes size, we reduced the transmitted LoRa data from 195 KB to 65 KB. The different settings used in the presented experiments are shown in Table 2.

TABLE 2: Scenario parameters

Spreading Factor	7, 8, 9, 10, 11, 12
Terrain	Line of Sight (LoS), Non Line of Sight (NLoS)
Distance (m)	15, 30, 60, 100, 200, 600

C. SIMULATION TOOL

The main scope of the simulation tool is to create a larger image dataset for the CNN models so that the reliability of the grape leaf diseases identification process is increased. To do so, the tool receives input from the pilot evaluation, and more specifically, the packet loss patterns, as well as an input from the PlantVillage database [33]. As a result, the simulator's output is a dataset of images with a reduced quality due to the packet loss effect. PlantVillage database contains images that were taken from experimental research stations associated with Land Grant Universities in the USA (Penn State, Florida State, Cornell, and others). The technicians collected the leaves by removing them from the plant and placing them over a paper sheet with a black background. As a result, every leaf in the dataset maintains high resolution, proximity views, and has the same orientation. The images were captured outside under full light using a digital camera. The original dataset contains 54.309 images from 14 crop species. For this study, we used a subset that consists of grape crops. Thus, 4.089 images are divided into four classes (Black rot, Esca, Leaf blight, and Healthy), three possible diseases, and a class representing healthy grape leaves.

D. SELECTED DL PRE-TRAINED MODELS

For the grape leaves disease identification task, CNN architectures are employed. To complement the simplicity of our approach, we adopted two lightweight but efficient state-of-the-art pre-trained CNN architectures, MobileNetV2 and ResNet50. The adopted architectures have been trained on the ILSVRC-2012 ImageNet dataset (1k classes/1.3 million images) [34]. The transferable parameters of these models enable them to converge faster and yield better results. Overall, we utilized the aforementioned models off-the-self using their trained weights as the starting point and fine-tuned them on the PlantVillage dataset.

In [35], the authors proposed a class of efficient models, MobileNets, for mobile and embedded vision applications, which achieves state-of-the-art performance on multiple tasks allowing efficient computing resources usage. MobileNetV1 introduced depthwise separable convolutions, which splits a kernel into two separate kernels: depthwise convolution applies a single convolutional filter for each input channel followed by a pointwise convolution, a 1×1 convolution to combine the outputs of the depthwise convolution. This factorization technique is computationally efficient and is a critical component of MobileNets architecture. The next generation of MobileNets, MobileNetV2 [36], is based on MobileNetV1 architecture. It significantly improves the accuracy of MobileNetV1 on various vision tasks, retaining the simplicity of its predecessor.

MobileNetV2 introduced the inverted residual block with the use of depthwise separable convolutions as useful blocks but with two new features: linear bottlenecks and shortcut residuals connections between the bottlenecks. This structure exploits the low-rank nature of the problem, creating efficient, lightweight layers. The inverted residual expands a low dimension vector, with the use of pointwise (1×1) convolutions to a higher-dimensional space followed by the activation function. In the sequel, a depth-wise convolution is applied, mapping the spatial correlations. After Rectified linear unit (Relu) [37], a 1×1 projection layer is adopted. The last operation is linear so that there is no further reduction in information. The input and output mappings are connected with a residual connection if and only if they have the same number of channels. The structure of this architecture provides a natural separation between the input/output domains of bottleneck and transformation layers. The network consists of 54 layers, has an input image size of 224×224 bytes, and has been trained using the ImageNet Dataset.

To tackle the vanishing gradient challenges that arose from training deep-neural networks, the authors in [31] proposed the ResNet CNN architecture. ResNet incorporates residual functions concerning layer inputs. Instead of approximating the function $H(x)$ that represents an underlying mapping to be learned, the authors enabled the layers to approximate a residual function $(F(x) := H(x) - x)$ using a parameter-free identity shortcut connections. ResNet architecture consists of two main blocks: the *Convolutional* and *Identity* blocks. Both Convolutional and identity blocks use standard convolution with 3×3 filters followed by BatchNormalization and ReLu activation function as their main components. Each block uses a three-layer stack with 1×1, 3×3 and 1×1 convolutions. The 1×1 convolutions reduce the input dimension, and the last restore it. The difference between these blocks lies in implementing the skip connection, as the convolutional block applies convolution operation on it. Identity blocks are essential to the network's efficiency and complexity. ResNets achieved state-of-the-art results in image recognition and object detection tasks.

IV. EVALUATION RESULTS

In this section, we performed the evaluation of the proposed system. Our evaluation consists of two main phases:

- Evaluation of image transmission using LoRa pilot: in this phase, 50 images were sent using our pilot and evaluated the performance of the LoRa communication link. We measured several performance parameters like the Packet Reception Ratio (PRR) and Over Air delays.
- Grape leaves disease identification: in this phase, we trained the proposed CNN models to identify disease patterns in grape leaves. We used our simulator to increase the number of images used and create images with similar characteristics as the images received during pilot evaluation. To do so, we import into the simulator the packet loss patterns extracted from the pilot evaluation and a dataset of around 4k images.

A. LORA PILOT EVALUATION

This subsection presents the performance evaluation of the scenario as described in the previous section. Fig. 2 shows the PRR obtained for Different Spreading Factors and distances. As expected, using a higher Spreading Factor, the packet loss

This article has been accepted for publication in a future issue of this journal, but has not been fully edited. Content may change prior to final publication. Citation information: DOI 10.1109/ACCESS.2021.3138050, IEEE Access

is decreased.For example, inn all the cases, when using SF = 12, 100% of the packets received. On the other hand, one can also easily observe that we can receive all the packets in short distances even with a lower Spreading Factor.

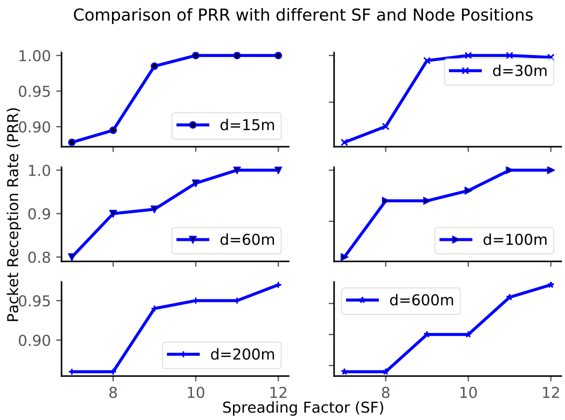

FIGURE 2: Comparison of PRR with different SF and distances

Tables 3 and 4 present the measured values of RSSI and SNR using SF = 7 and SF = 12, respectively. Based on the results, we observe that the RSSI and SNR depend on the distance of the nodes. Furthermore, the structure of the field between the node and gateway affects the results significantly. For example, node 4 shows a lower RSSI value compared to node 5, even though its distance from the gateway is half. This is due to the obstructed path of node four and the gateway. Furthermore, one observes that when using SF = 7, a higher RSSI value for the same node is obtained when compared to SF = 12. Finally, regarding SNR, it is shown that there is a small increase in SNR when increasing the spreading Factor. This is in line with the expected behavior since higher SF increases the SNR, transmission range, packet airtime and decreases the data rate.

TABLE 3: RSSI and SNR ranges for nodes using SF = 7

Node ID	Distance	RSSI Average	RSSI Range	SNR Average	SNR Range
1	15	-81	-79 to -107	9	-11 to 11
2	30	-89	-85 to -92	9	4 to 12
3	60	-90	-87 to -93	9	5 to 11
4	100	-101	-95 to -109	5	-7 to 9
5	200	-95	-92 to -103	8	4 to 11
6	600	-103	-99 to -108	4	-3 to 6

TABLE 4: RSSI and SNR ranges for nodes using SF = 12

Node ID	Distance	RSSI Average	RSSI Range	SNR Average	SNR Range
1	15	-85	-78 to -100	9	2 to 13
2	30	-90	-88 to -94	9	7 to 11
3	60	-91	-83 to -95	9	6 to 10
4	100	-102	-94 to -105	5	-6 to 9
5	200	-96	-89 to -101	9	5 to 11
6	600	-104	-96 to -108	5	-3 to 8

Figs. 3 and 4 illustrate the relationship between the RSSI, SNR and PRR. In both cases, the SNR values recorded by nodes follow the fluctuation trend of corresponding RSSI values. Also, the behavior of RSSI and SNR affects the PRR, especially when using SF = 7. In the case of SF = 12, it is shown that even under RSSI fluctuations, the specific setup was able to deliver 100% of the messages.

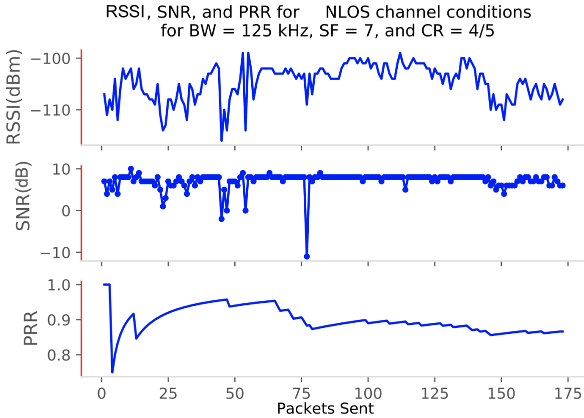

FIGURE 3: RSSI, SNR, and PRR for in NLOS channel conditions for BW = 125 kHz, SF = 7, and CR = 4/5.

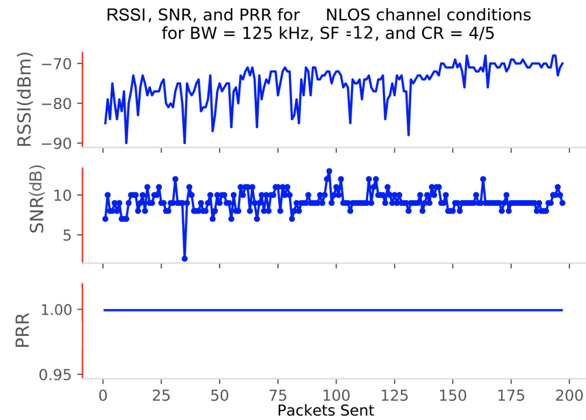

FIGURE 4: RSSI, SNR, and PRR for in NLOS channel conditions for BW = 125 kHz, SF = 12, and CR = 4/5.

Table 5 depicts Over the Air delays with different Spreading Factors for all nodes. In our scenarios, we use the same payload size for SF7 - SF9, which is 85 bytes and 51 bytes for SF10 - SF12. The size of the payload is based on the maximum image size, which is 255$\times$255 bytes, and the maximum payload size for each Spreading Factor. Based on the evaluation results, the air delay depended mostly on the Spreading Factor and not on the distance or obstacles in the communication path. It is observed that lower Spreading Factors lead to less delay, and the delay increases exponentially as the Spreading Factor increases. The most important conclusion is that a Spreading Factor of 7 reduces the time elapsed during transfer and is more applicable for scenarios where we want to transfer data like an image. In general, higher transmission speeds will lead to less battery usage and gateway utilization.

TABLE 5: Measured Over the Air delays with different Spreading Factor and node distance

Node distance=15 m		Node distance=30 m		Node distance=60 m	
SF	Over the Air (ms)	SF	Over the Air (ms)	SF	Over the Air (ms)
7	170	7	170	7	171
8	298	8	299	8	299
9	534	9	534	9	535
10	699	10	700	10	700
11	1560	11	1561	11	1563
12	2794	12	2795	12	2795
Node distance=100 m		Node distance=200 m		Node distance=600 m	
SF	Over the Air (ms)	SF	Over the Air (ms)	SF	Over the Air (ms)
7	170	7	171	7	171
8	298	8	298	8	299
9	535	9	535	9	536
10	700	10	701	10	701
11	1562	11	1563	11	1563
12	2795	12	2795	12	2795

Fig. 5 shows the effect of the external temperature on RSSI. It is clear that as the temperature increases, the RSSI decreases. This is in line with [13] which shows that the effect of temperature on LoRa's packet delivery can be quite severe.

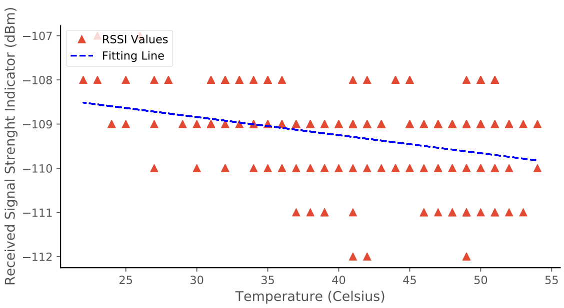

FIGURE 5: Temperature effect on RSSI

Finally, Table 6 depicts the number of total packets required to be sent using different image sizes as well as the total time required to send an image and the total number of images that the protocol can send to the gateway. Based on Table 6, we observed that the maximum number of images are sent using Spreading Factor 7 since the Over the Air delay is the minimum compared to the other Spreading Factors. All these results are based on the limitation of 1% (36sec/hour) of the duty cycle for the sending node. For example, an image with size 255×255 is equal to 65025 bytes. In our case, when using SF = 7, the payload of the packet is equal to 85 bytes, which means 765 packets are required to be sent.

B. GRAPE LEAVES DISEASE IDENTIFICATION

The following procedure considers the intensity values of the pixels, which are calculated as the mean $Gr[x, y]$ of the pixels' RGB values: $Gr[x, y] = (R[x, y] + G[x, y] + B[x, y])/3$. The calculated intensity value replaces all the pixel $[x, y]$ R, G, and B values. This modification allows us to adopt the pre-trained off-the-shelf network without further adjustments. The last layer of the network is replaced with one corresponding to the number of possible classes for classification. The networks are trained using Adam optimizer. We use batch size 32 and EarlyStopping limit of 10 epochs. The initial learning rate is 1×10^{-4} and is divided by ten every five epochs if there is no improvement in the validation set. We experimented with various image sizes and trained the models for two different setups: 1) using original images and 2) using random augmentations on images (rotation, horizontal flip, and vertical flip). In addition, we adopted different values of PRR for every image size, resulting in partly corrupted images as they contain missing values in proportion to PRR value. To reconstruct the image, the missing values are replaced with 0's. Fig. 6 depicts sample images - one from each class, while Fig. 7 depicts the visual corruption on images under different LoRa's packet loss levels.

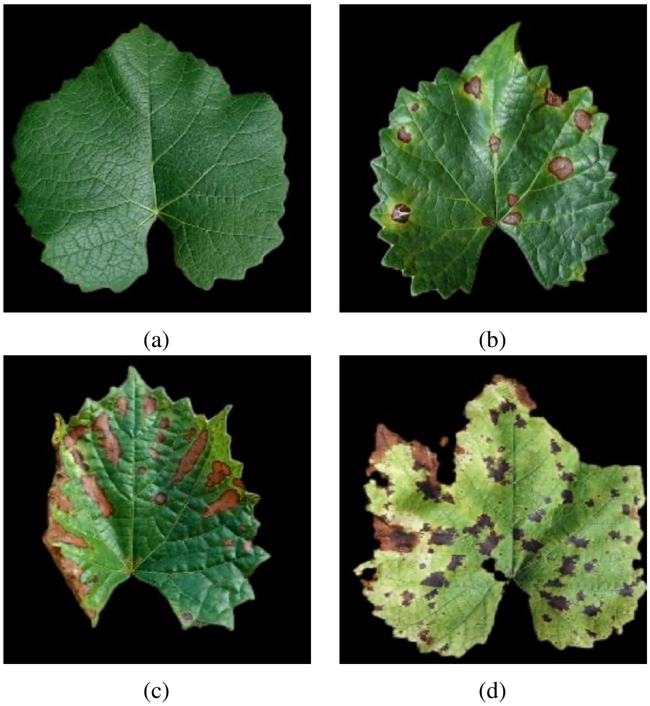

FIGURE 6: Sample images from the employed dataset: (a) Healthy Leaf, (b) Black rot, (c) Esca, and (d) Leaf blight.

1) Results

Once again, it is critical to emphasize the implementation's goal. The studies were carried out to provide us with an understanding of standard CNN architectures' robustness to considerably noisy data due to transmission packet loss and their suitability for such tasks. We did not utilize rigorous hyper-parameter tuning or complicated CNN architectures as we focused on comparing the models' prediction power when the quality of images is significantly altered. In this regard, the performance degradation across the setups is the most essential factor.

This article has been accepted for publication in a future issue of this journal, but has not been fully edited. Content may change prior to final publication. Citation information: DOI 10.1109/ACCESS.2021.3138050, IEEE Access

TABLE 6: LoRa with different image sizes using different Spreading Factors

	SF = 7			SF = 8		
Image Size	Packets	Total time (ms)	Images/day	Packets	Total time (ms)	Images/day
255x255	765	130050	6	765	227970	3
128x128	256	43520	19	256	76288	11
64x64	64	10880	79	64	19072	45
32x32	16	2720	317	16	4768	181
	SF = 9			SF = 10		
Image Size	Packets	Total time (ms)	Images/day	Packets	Total time (ms)	Images/day
255x255	765	408510	2	1275	892500	0
128x128	256	136704	6	322	225400	3
64x64	64	34176	25	81	56700	15
32x32	16	8544	101	21	14700	58
	SF = 11			SF = 12		
Image Size	Packets	Total time (ms)	Images/day	Packets	Total time (ms)	Images/day
255x255	1275	1990275	0	1275	3563625	0
128x128	322	502642	1	322	899990	0
64x64	81	126441	6	81	226395	3
32x32	21	32781	26	21	58695	14

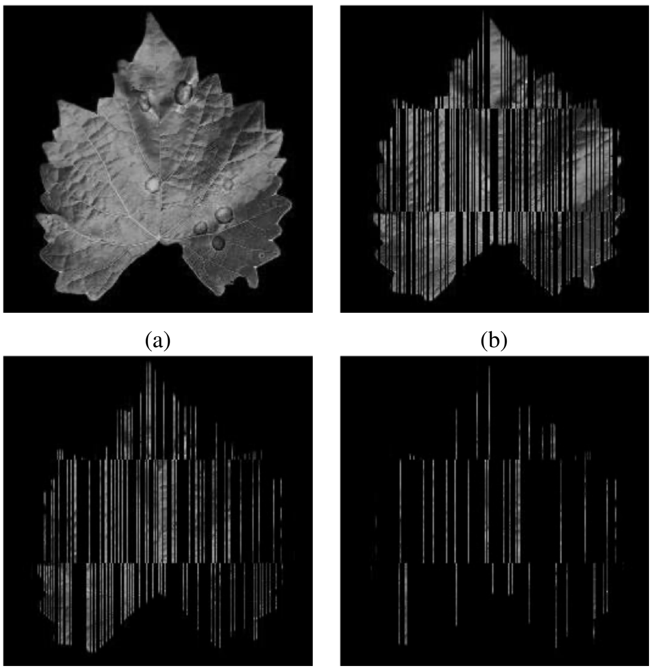

(a) (b) (c) (d)

FIGURE 7: Image Corruption under different Lora's packet loss levels: (a) 0%, (b) 25%, (b) 50% and (d) 75%

Table 8 and 9 present the classification accuracy of ResNet50, with and without augmentation. It is noticeable that the application of augmentation provides a subtle improvement in all training scenarios. In both setups, the network is robust to packet loss on the condition such that the original image's dimensions are preserved. Therefore, CNN can handle missing pixel values resulting from transmission errors. While the downscaling process introduces another noise factor in addition to packet loss, it decreases the required channel bandwidth, significantly enabling LoRa to transmit images effectively when the bandwidth is narrow.

It is also worth noting that control experiments have also been conducted by employing the MobileNetV2 (as these are illustrated in Table 7). One can easily observe that the performance of ResNet50 outperforms the one reported by MobileNetV2 without compromising efficiency. In summary, CNNs employment is crucial to combat the challenge of narrow bandwidth due to long-distance transmission.

Overall, we attempt to present some widely used CNN architectures which, although they have been used in identifying crops diseases, to the best of our knowledge, have not been adopted in a similar setting where data quality is seriously affected by network's limitations. Furthermore, in the absence of packet loss and while using the original picture dimensions, the performance of the used CNNs is consistent with the literature [38] [39]. Even though the findings are not directly comparable due to the random test split, they are in the same ballpark.

TABLE 7: MobileNetV2

Image Size (Bytes)	**255×255**	**128×128**	**64×64**	**32×32**
PRR 100%	99.54	98.68	94.88	87.63

TABLE 8: Classification accuracy of ResNet50 without augmentation

Image Size (Bytes)	**255×255**	**128×128**	**64×64**	**32×32**
PRR 100%	99.65	98.86	95.9	88.75
PRR 75%	98.06	97.27	92.15	86.64
PRR 50%	97.15	94.31	90.3	85.0
PRR 25%	94.77	92.95	86.70	74.65
PRR 10%	91.81	87.72	81.68	66.20

2) Visualization

We utilized the Grad-CAM algorithm to visualize the decisions of CNN's output layer. This allows us to identify exactly which part of the leaf is associated with a particular classification. Grad-CAM [40] uses the gradient information that flows into the last convolutional layer of CNN to assign

This article has been accepted for publication in a future issue of this journal, but has not been fully edited. Content may change prior to final publication. Citation information: DOI 10.1109/ACCESS.2021.3138050, IEEE Access

TABLE 9: Classification accuracy of ResNet50 with augmentation

Image Size (Bytes)	255×255	128×128	64×64	32×32
PRR 100%	99.77	99.02	96.31	89.2
PRR 75%	98.33	97.61	92.48	87.2
PRR 50%	97.27	94.53	91.25	85.56
PRR 25%	94.97	93.27	87.86	75.45
PRR 10%	92.2	89.07	82.72	66.8

significance values to each neuron. Fig. 8 presents Grad-CAM visualizations of leaf images for different PRR values. Blue regions represent the parts of the image where the CNN's attention is focused and influence the final classification decision. According to the visualization findings, the spot region of the disease is highly activated. This is how the network distinguishes between various diseases of the grape leaves. It is clear that as the PRR declines, the attention drifts apart. In particular, when PRR is equal to 10%, the model focuses more on the shape of the leaf as most of the diseased spots are missing due to packet loss. Overall, the findings of this experiment reveal that the model can identify the characteristics of each disease spot effectively in noisy scenarios.

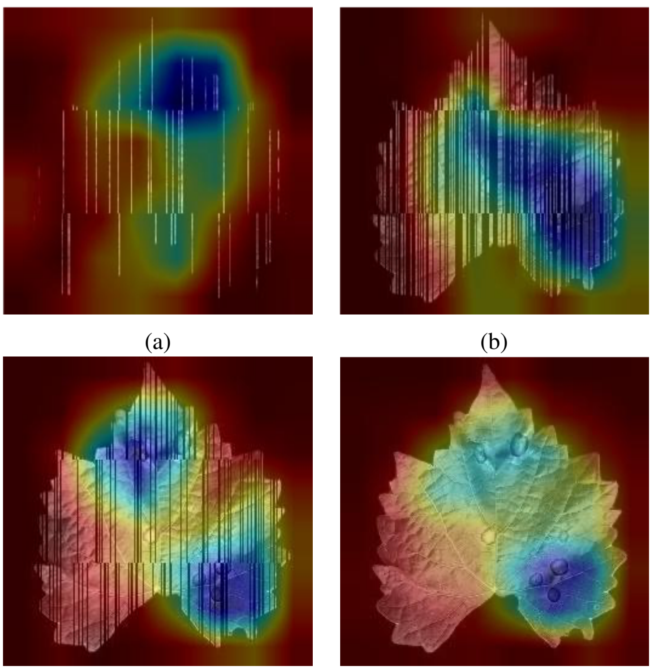

(a) (b) (c) (d)

FIGURE 8: Grad-CAM visualizations of leaf images for different PRR values. (a) 10%, (b) 50%, (c) 75% and (d) 100%

V. CONCLUSION AND FUTURE WORK

LoRa protocol was meant to be used for applications requiring long-distance, low data rate, and low power consumption. In addition, limitations like the maximum duty cycle of 1%, which means that the node can only be active for 36 seconds per hour, make LoRa unsuitable for image transmission. In this paper, we demonstrated a grape leaf diseases scenario using images that were sent with LoRa. To make this possible, we reduced the size of the transmitted image by transforming the images to grayscale. Furthermore, we evaluated the CNN model using images with packet losses so that to test how reduced quality images affect the identification of the grape leaf diseases. Thus, we can conclude that image transmission using LoRa could be possible, especially when the quality of the received images does not affect the performance of the application, in our scenario, the grape leaf diseases identification. In our case, even when 50% of the image was lost, we managed to identify the grape leaf diseases efficiently. As future work, we plan to use more LoRa gateways to operate in multiple channels such that the number of images sent by each LoRa node is increased, which in turn improves the leaves diseases detection process.

REFERENCES

[1] A. Augustin, J. Yi, T. Clausen, and W. M. Townsley, "A study of lora: Long range low power networks for the internet of things," Sensors, vol. 16, no. 9, 2016.

[2] L. Doitsidis, G. N. Fouskitakis, K. N. Varikou, I. I. Rigakis, S. A. Chatzichristofis, A. K. Papafilippaki, and A. E. Birouraki, "Remote monitoring of the bactrocera oleae (gmelin) (diptera: Tephritidae) population using an automated mcphail trap," Comput. Electron. Agric., vol. 137, pp. 69–78, 2017. [Online]. Available: https://doi.org/10.1016/j.compag.2017.03.014

[3] A. Khalifeh, K. A. Aldahdouh, K. A. Darabkh, and W. Al-Sit, "A survey of 5g emerging wireless technologies featuring lorawan, sigfox, nb-iot and lte-m," in 2019 International Conference on Wireless Communications Signal Processing and Networking (WiSPNET), 2019, pp. 561–566.

[4] O. Khutsoane, B. Isong, and A. M. Abu-Mahfouz, "Iot devices and applications based on lora/lorawan," in Proc. IEEE IECON 2017- 43rd Annu. Conf. IEEE Ind. Electron. Soc., janua, Nov 2017, pp. 6107–6112.

[5] M. A. Ertürk, M. A. Aydın, M. T. Büyükakkaşlar, and H. Evirgen, "A survey on lorawan architecture, protocol and technologies," Future Internet, vol. 11, no. 10, 2019. [Online]. Available: https://www.mdpi.com/1999-5903/11/10/216

[6] S. Wang, Y. Chen, T. Chen, C. Chang, Y. Cheng, C. Hsu, and Y. Lin, "Performance of lora-based iot applications on campus," in 2017 IEEE 86th Vehicular Technology Conference (VTC-Fall), Sep. 2017, pp. 1–6.

[7] J. Petajajarvi, K. Mikhaylov, A. Roivainen, T. Hanninen, and M. Pettissalo, "On the coverage of lpwans: range evaluation and channel attenuation model for lora technology," in 2015 14th International Conference on ITS Telecommunications (ITST), Dec 2015, pp. 55–59.

[8] C.-L. Hsieh, Z. Ye, C.-K. Huang, Y.-C. Lee, C. Sun, T.-H. Wen, J.-Y. Juang, and J.-A. Jiang, "A vehicle monitoring system based on the lora technique," 2017.

[9] Y. Ma and J. Chen, "Toward intelligent agriculture service platform with lora-based wireless sensor network," in 2018 IEEE International Conference on Applied System Invention, April 2018, pp. 204–207.

[10] D. Yim, J. Chung, Y. Cho, H. Song, D. Jin, S. Kim, S. Ko, A. Smith, and A. Riegsecker, "An experimental lora performance evaluation in tree farm," in 2018 IEEE Sensors Applications Symposium (SAS), March 2018, pp. 1–6.

[11] J. Bauer and N. Aschenbruck, "Towards a low-cost rssi-based crop monitoring," ACM Trans. Internet Things, vol. 1, no. 4, Jun. 2020. [Online]. Available: https://doi.org/10.1145/3393667

[12] D. Eridani, E. D. Widianto, R. D. O. Augustinus, and A. A. Faizal, "Monitoring system in lora network architecture using smart gateway in simple lora protocol," in 2019 International Seminar on Research of Information Technology and Intelligent Systems (ISRITI), Dec 2019, pp. 200–204.

[13] C. A. Boano., M. Cattani., and K. Römer., "Impact of temperature variations on the reliability of lora - an experimental evaluation," in Proceedings of the 7th International Conference on Sensor Networks - Volume 1: SENSORNETS,, INSTICC. SciTePress, 2018, pp. 39–50.

[14] E. D. Widianto, M. S. M. Pakpahan, A. A. Faizal, and R. Septiana, "Lora qos performance analysis on various spreading factor in indonesia," in 2018 International Symposium on Electronics and Smart Devices (ISESD), Oct 2018, pp. 1–5.

[15] C. Bouras, A. Gkamas, V. Kokkinos, and N. Papachristos, "Using lora technology for iot monitoring systems," in 2019 10th International Conference on Networks of the Future (NoF), Oct 2019, pp. 134–137.

[16] C. Pham, "Low-cost, low-power and long-range image sensor for visual surveillance," in Proceedings of the 2nd Workshop on Experiences in the Design and Implementation of Smart Objects, ser. SmartObjects '16. New York, NY, USA: Association for Computing Machinery, 2016, p. 35–40. [Online]. Available: https://doi.org/10.1145/2980147.2980156

[17] R. Kirichek, V.-D. Pham, A. Kolechkin, M. Al-Bahri, and A. Paramonov, "Transfer of multimedia data via lora," in Internet of Things, Smart Spaces, and Next Generation Networks and Systems, O. Galinina, S. Andreev, S. Balandin, and Y. Koucheryavy, Eds. Cham: Springer International Publishing, 2017, pp. 708–720.

[18] A. Jebril, A. Sali, A. Ismail, and M. Rasid, "Overcoming limitations of lora physical layer in image transmission," Sensors, vol. 18, no. 10, p. 3257, Sep 2018. [Online]. Available: http://dx.doi.org/10.3390/s18103257

[19] C. Pham, "Robust csma for long-range lora transmissions with image sensing devices," in 2018 Wireless Days (WD), 2018, pp. 116–122.

[20] M. Ji, J. Yoon, J. Choo, M. Jang, and A. Smith, "Lora-based visual monitoring scheme for agriculture iot," in 2019 IEEE Sensors Applications Symposium (SAS), March 2019, pp. 1–6.

[21] A. Selvaraj, N. Shebiah, S. Ananthi, and S. Varthini, "Detection of unhealthy region of plant leaves and classification of plant leaf diseases using texture features," Agricultural Engineering International: CIGR Journal, vol. 15, pp. 211–217, 01 2013.

[22] J. G. A. Barbedo, L. V. Koenigkan, and T. T. Santos, "Identifying multiple plant diseases using digital image processing," Biosystems engineering, vol. 147, pp. 104–116, 2016.

[23] S. Sakthi, M. Palaniappan, D. Thenmozhi, and Vatsala, "Grape leaf disease identification using machine learning techniques," 2019, pp. 1–6.

[24] U. Singh, A. Srivastava, D. Chauhan, and A. Singh, "Computer vision technique for detection of grape esca (black measles) disease from grape leaf samples," 02 2020, pp. 110–115.

[25] M. D. Zeiler and R. Fergus, "Visualizing and understanding convolutional networks," ArXiv, vol. abs/1311.2901, 2014.

[26] A. Razavian, H. Azizpour, J. Sullivan, and S. Carlsson, "Cnn features off-the-shelf: An astounding baseline for recognition," 2014 IEEE Conference on Computer Vision and Pattern Recognition Workshops, pp. 512–519, 2014.

[27] S. Zhang, S. Zhang, C. Zhang, X. Wang, and Y. Shi, "Cucumber leaf disease identification with global pooling dilated convolutional neural network," Computers and Electronics in Agriculture, vol. 162, pp. 422–430, 2019.

[28] P. Sharma, Y. P. S. Berwal, and W. Ghai, "Performance analysis of deep learning cnn models for disease detection in plants using image segmentation," Information Processing in Agriculture, 2019.

[29] S. Huang, W. Liu, F. Qi, and K. Yang, "Development and validation of a deep learning algorithm for the recognition of plant disease," in 2019 IEEE 21st International Conference on High Performance Computing and Communications; IEEE 17th International Conference on Smart City; IEEE 5th International Conference on Data Science and Systems (HPCC/SmartCity/DSS), 2019, pp. 1951–1957.

[30] Q. Liang, S. Xiang, Y. Hu, G. Coppola, D. Zhang, and W. Sun, "Pd2se-net: Computer-assisted plant disease diagnosis and severity estimation network," Computers and electronics in agriculture, vol. 157, pp. 518–529, 2019.

[31] K. He, X. Zhang, S. Ren, and J. Sun, "Deep residual learning for image recognition," in Proceedings of the IEEE conference on computer vision and pattern recognition, 2016, pp. 770–778.

[32] A. Anastasiou, P. Christodoulou, K. Christodoulou, V. Vassiliou, and Z. Zinonos, "Iot device firmware update over lora: The blockchain solution," in 2020 16th International Conference on Distributed Computing in Sensor Systems (DCOSS), 2020, pp. 404–411.

[33] S. P. Mohanty, D. P. Hughes, and M. Salathé, "Using deep learning for image-based plant disease detection," Frontiers in plant science, vol. 7, p. 1419, 2016.

[34] J. Deng, W. Dong, R. Socher, L. Li, Kai Li, and Li Fei-Fei, "Imagenet: A large-scale hierarchical image database," in 2009 IEEE Conference on Computer Vision and Pattern Recognition, 2009, pp. 248–255.

[35] A. G. Howard, M. Zhu, B. Chen, D. Kalenichenko, W. Wang, T. Weyand, M. Andreetto, and H. Adam, "Mobilenets: Efficient convolutional neural networks for mobile vision applications," arXiv preprint arXiv:1704.04861, 2017.

[36] M. Sandler, A. Howard, M. Zhu, A. Zhmoginov, and L.-C. Chen, "Mobilenetv2: Inverted residuals and linear bottlenecks," in Proceedings of the IEEE conference on computer vision and pattern recognition, 2018, pp. 4510–4520.

[37] X. Glorot, A. Bordes, and Y. Bengio, "Deep sparse rectifier neural networks," in AISTATS, 2011.

[38] N. Gangwar, D. Tiwari, A. Sharma, M. Ashish, and A. Mittal, "Grape leaf disease classification using transfer learning," 2020.

[39] K. Aravind, P. Raja, R. Aniirudh, K. Mukesh, R. Ashiwin, and G. Vikas, "Grape crop disease classification using transfer learning approach," Springer, pp. 1623–1633, 2018.

[40] R. R. Selvaraju, M. Cogswell, A. Das, R. Vedantam, D. Parikh, and D. Batra, "Grad-cam: Visual explanations from deep networks via gradient-based localization," in Proceedings of the IEEE international conference on computer vision, 2017, pp. 618–626.

ZINON ZINONOS received his diploma in Computer Engineering from the Computer Engineering and Informatics Department (CEID) of the University of Patras, Greece, in 2005, and the M.Sc and Ph.D. degrees from Computer Science Department, University of Cyprus, in 2008 and 2013, respectively, all in computer science. Currently, he is an Assistant Professor at the Computer Science Department of Neapolis University. He is also the Assistant Director of the Intelligent Systems Laboratory (ISL) at NUP. His research interests include Internet of Things (IoT), wireless, ad hoc, and sensor networks, mobility management in low power devices, adaptive topology control, computer communication networks, blockchain for IoT, intelligent systems, implementation of real-time monitoring and control systems, and energy efficiency.

SOCRATIS GKELIOS received his diploma degree from the Department of Electrical and Computer Engineering, Democritus University of Thrace, in 2019. He is currently a Ph.D. candidate in Computer Science at the same department and a Research Assistant at the Centre for Research and Technology Hellas (CE.R.T.H.), Information Technologies Institute (ITI). His research is focused on computer vision, image retrieval, and deep learning.

This article has been accepted for publication in a future issue of this journal, but has not been fully edited. Content may change prior to final publication. Citation information: DOI 10.1109/ACCESS.2021.3138050, IEEE Access

ALA' KHALIFEH received the Ph.D. degree in Electrical and Computer Engineering from the University of California, Irvine -the USA in 2010. He is currently an Associate Professor in the Communication Engineering department at the German Jordanian University and the department chair. Dr. Khalifeh is the recipient of the Fulbright scholarship (2005-2007) sponsored by the Bureau of Educational and Cultural Affairs of the United States Department of State and the University of California Pedagogical fellowship for his excellent teaching and leadership skills. He has received numerous academic and technical awards, such as The Young AFCEA 40 Under 40 winners. The German Jordanian University award for the industrial relationship Jul 2016 and the German Jordanian University Excellence in Research Award, Sep 2015. His research is in communications technology, signal processing, and networking, emphasizing optimal resource allocations for multimedia transmission over wired and wireless networks, VoIP, E-health applications, speech, video, and audio signal processing.

DIOFANTOS G. HADJIMITSIS is the Managing Director of the "ERATOSTHENES Centre of Excellence" (www.eratosthenes.org.cy) of the Cyprus University of Technology and full Professor at the Department of Civil Engineering and Geomatics of the Cyprus University of Technology. He is the head of the Remote Sensing and GeoEnvironment Lab. He was the Vice-Rector of Academic Affairs of the Cyprus University of Technology from 2016 to 2019. He is the Coordinator of the Excelsior H2020 Widespread Teaming project www.excelsior2020.eu (38 million euros funding). Diofantos is a member of the Cyprus Scientific and Technical Chamber (). In the past, he has worked at the University of Surrey (UK), University of Southampton (UK), and Frederick University (Cyprus) as well in the industrial sector in the fields of remote sensing, geo-information, and civil engineering. He has authored more than 300 research publications in peer-reviewed journals, conference proceedings, chapters in books, and technical reports. His research group is the biggest group at the Cyprus University of Technology, consisting of 60 active researchers

YIANNIS S. BOUTALIS received the diploma of Electrical Engineer in 1983 from Democritus University of Thrace (DUTH), Greece and the Ph.D. degree in Electrical and Computer Engineering in 1988 from the Computer Science Division of National Technical University of Athens, Greece. Since 1996, he has served as a faculty member at the Department of Electrical and Computer Engineering, DUTH, Greece, where, after serving as a Lecturer, Assistant Professor, and Associate Professor, he is currently Professor and director of the Automatic Control Systems Robotics Lab, as well as Head of the Department. In the past, he served as an assistant visiting professor at the University of Thessaly (PD 407), Greece, and as a visiting professor (under contract) in the Air Defense Academy of General Staff of air forces of Greece. His current research interests are focused on the development of Computational Intelligence Techniques with applications in Control, Renewable Power Generation, Electric Machines, Robotics, Pattern Recognition, Signal and Image Processing Problems.

SAVVAS A. CHATZICHRISTOFIS received his Diploma as well as his Ph.D. degree (with honors) from the Department of Electrical and Computer Engineering, Democritus University of Thrace, Greece. Since 2017, he has been a Faculty Member with the Department of Computer Science, Neapolis University Pafos. He is currently an Associate Professor and the Director of the Intelligent Systems Laboratory (ISL). His research focuses on the intersection of Artificial Intelligence, Computer Vision, and Robotics. His scientific interests lie in the following fields: visual feature extraction, image analysis, matching, indexing and retrieval, SLAM, and Educational Robotics. He has over 13 years of solid experience reporting more than 85 publications in these fields. For his research contribution, he has received several distinctions, grants, scholarships, and awards.